AD-A032 049 ARMY ELECTRONICS COMMAND FORT MONMOUTH N J F/G 17/5
ELECTRON SOURCES FOR FUTURE IMAGE TUBES.(U)
JUN 76 T L JONES
UNCLASSIFIED ECOM-7054 NL

1 OF 1
ADA032049

END
DATE FILMED
1 -77

AD

Research and Development Technical Report

ECOM–7054

ELECTRON SOURCES FOR FUTURE IMAGE TUBES

June 1976

Approved for public release; distribution unlimited.

ECOM

UNITED STATES ARMY ELECTRONICS COMMAND . FORT MONMOUTH, NJ

Destroy this report when no longer needed.
Do not return it to the originator.

The citation in this report of trade names of commercially available products does not constitute official endorsement or approval of the use of such products.

UNCLASSIFIED

SECURITY CLASSIFICATION OF THIS PAGE *(When Data Entered)*

REPORT DOCUMENTATION PAGE	READ INSTRUCTIONS BEFORE COMPLETING FORM
1. REPORT NUMBER: ECOM-7054	2. GOVT ACCESSION NO. —	3. RECIPIENT'S CATALOG NUMBER
4. TITLE *(and Subtitle)*: ELECTRON SOURCES FOR FUTURE IMAGE TUBES	5. TYPE OF REPORT & PERIOD COVERED: Work Unit Final Report, Sep 71 – May 73
	6. PERFORMING ORG. REPORT NUMBER
7. AUTHOR(s): Terry L. Jones	8. CONTRACT OR GRANT NUMBER(s)
9. PERFORMING ORGANIZATION NAME AND ADDRESS: Night Vision Laboratory, DRSEL-NV-FIR, Fort Belvoir, Virginia 22060	10. PROGRAM ELEMENT, PROJECT, TASK AREA & WORK UNIT NUMBERS: 61102A, 31B, 06, 028CJ
11. CONTROLLING OFFICE NAME AND ADDRESS: Night Vision Laboratory, DRSEL-NV-FIR, Fort Belvoir, Virginia 22060	12. REPORT DATE: June 1976
	13. NUMBER OF PAGES: 38
14. MONITORING AGENCY NAME & ADDRESS *(if different from Controlling Office)*	15. SECURITY CLASS. *(of this report)*: Unclassified
	15a. DECLASSIFICATION/DOWNGRADING SCHEDULE

16. DISTRIBUTION STATEMENT *(of this Report)*

Approved for public release; distribution unlimited.

17. DISTRIBUTION STATEMENT *(of the abstract entered in Block 20, if different from Report)*

16 1T061102A31B

18. SUPPLEMENTARY NOTES

17 06

19. KEY WORDS *(Continue on reverse side if necessary and identify by block number)*

20. ABSTRACT *(Continue on reverse side if necessary and identify by block number)*

Several electron sources were investigated for use in far infrared image tubes in an effort to find or develop sources which had sharp cutoffs in their electron energy distribution curves (EDC's). An angular electron energy analyzer system was fabricated and used to evaluate not only EDC's but also their dependence on emission angle. Primary experimental attention was directed at two electrostatic filtering techniques – 127° cylindrical and hemispherical – and three emitters – miniature field-emitter tips, tin oxide thin films, and negative electron affinity (NEA) gallium phosphide photoemitters. None of these were developed sufficiently for use in

(Continued)

DD FORM 1 JAN 73 1473 EDITION OF 1 NOV 65 IS OBSOLETE

UNCLASSIFIED 037620

SECURITY CLASSIFICATION OF THIS PAGE *(When Data Entered)*

(Block 20 (Cont'd))

image tube applications. However, the field-emitter tips and NEA emitter look promising for improving the contrast enhancement in future image tubes.

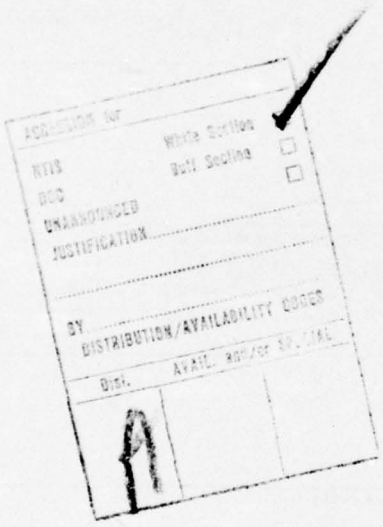

PREFACE

This report is a summary of an investigation by the Exploratory Techniques Team, Far Infrared Technical Area, *Night Vision Laboratory*, *Fort Belvoir*, *Virginia*. Most of the work was done under work unit 045, "Monoenergetic Electron Sources," which was initiated in September 1971 and was terminated in May 1973. This work unit was a part of Project 1T061102A31B, Task 06. Terry L. Jones was the principal investigator in-house and also the COTR on the external contracts which supported this internal work unit. Further details on internal work may be found in laboratory notebooks NVL-53-69 and NVL-7-72. Useful contractor reports are listed in the bibliography.

CONTENTS

ILLUSTRATIONS

ELECTRON SOURCES FOR FUTURE IMAGE TUBES

1. INTRODUCTION

A major problem in most types of far infrared imaging tubes is to provide an output with sufficient contrast for an observer to see the image of objects in the scene. Under ideal conditions, the eye can see an image with only 4% contrast; but, when viewing small or faint images, 50% contrast may be required. Since the far infrared signal information from many scenes is less than 1 percent above the ambient background radiation, the background must often be suppressed before an observable image can be displayed. By using electron beams which are nearly monoenergetic, tubes can be built which discriminate against "background electrons" and, as a result, greatly improve the contrast in the image presented to an observer.

As an example, suppose an ideal monoenergetic electron emitter is used in a velocity-selector, direct-view tube (Figure 1). Assume that the electrons are emitted normally with essentially zero kinetic energy. The incoming infrared image generates a potential-difference image in the detecting layer, V_s, and also at the emitting surface, V_e's, i.e., areas receiving signal information are at a lower voltage than areas receiving only background radiation. As a result, the emitted electrons are drawn through the extractor grid with differing energies, ϵ's, due to the potential difference generated by the infrared signal. If the voltage, V_s, of the velocity-selector grid is set only infinitesimally more negative than the voltage, V_{eb}, of the emitting surface elements where only background radiation is absorbed and no signal potential is generated, then only electrons from areas which have a signal-generated potential at the surface, V_e, more negative than V_s will have sufficient energy to pass through the selector grid. In other words, electrons from all elements with $V_e < V_s$ will be transmitted, and electrons from elements with $V_e \geq V_s$ will be reflected. This ideal tube has infinite contrast enhancement because the infrared background is totally suppressed electronically.

Unfortunately, there are several practical limitations which make the velocity-selector tube, and also other image tubes, far from ideal. In the selector tube, field distortion near the grids, work function variations on the velocity-selector grid, and non-normal incidence of electrons approaching the selector grid are major problems. Field distortion near the grids can be improved by using fine grids and weak electric fields; work function variations can be limited to less than 50 mV by proper selection of materials; and electron angle of incidence at the velocity selector grid can be improved by employing electron sources which emit most of their electrons normal to the emitter surface or by using collimating lenses or small-acceptance apertures. However, there are some trade-offs involved in applying these solutions; and, as a result, they are of only limited value.

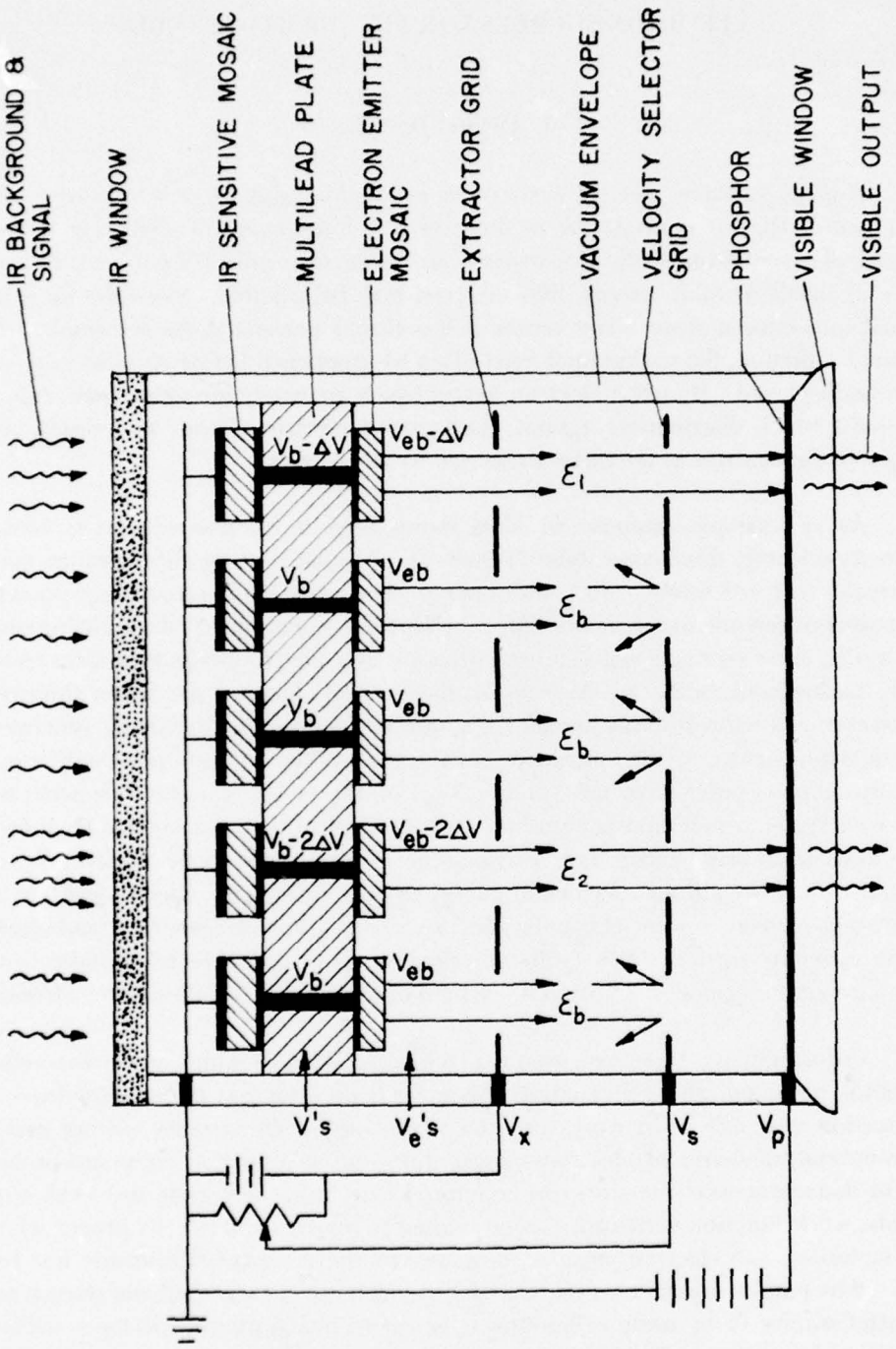

Figure 1. An idealized, infrared, direct-view tube showing total suppression of the infrared background by use of a velocity-selector grid and a monoenergetic electron emitter.

In addition to the three problems just mentioned, the nonuniformity of the sensing layer must be considered in all image tubes. If an electron source with 50 meV energy spread and near-normal emission were available, the sensing layer uniformity required to take full advantage of it is just barely within reach of today's technology. Consequently, for tube applications, it is useless to design electron sources which have energy spreads less than about 50 meV.

In the preceding paragraph, the energy spread was described by a rather vague term – a meV range of electron energies without any indication of how this was to be measured. Although this is common practice, the energy spread of electron sources can only be accurately described by electron energy distribution curves (EDC's). In cases where such a detailed description is not necessary, several less precise but often adequate descriptions have come into use. Some of the more common ones are full EDC width at half maximum (FWHM), half EDC width at half maximum (HWHM), EDC width containing all but 10% of the least energetic and 10% of the most energetic electrons (10-90%), most probable energy and cathode temperature,[1] and effective electron temperature. Unfortunately, none of these are very useful in this discussion.

For image tube applications, the most important parameter affecting the contrast enhancement is not the energy spread itself but the shape of the sides of the energy-distribution curve. In tubes like the velocity-selector tube or the standard vidicon, the primary concern is the high-energy side of the EDC; whereas, in mirror tubes or return-beam vidicons, the low-energy side is more crucial.

The contrast enhancement is propositional to $\frac{1}{I}\left|\frac{dI}{dv}\right|$, where I is the current and v, the signal voltage (the V_e's in the tube shown in Figure 1). The contrast enhancement can be related to the shape of the sides of the EDC in the following way: Take $N(\epsilon)$ as the number of electrons per second per unit energy interval from the source. Then the sides of the EDC can be approximated by exponentials in terms of the electron energy, ϵ, the magnitude of the electron charge, q, and constants, N_o and α: $N_h(\epsilon) \approx N_{ho} e^{\frac{\alpha\epsilon}{q}}$, $(\alpha < 0)$ for the high-energy side, and $N_\ell(\epsilon) \approx N_{\ell o} e^{\frac{\alpha\epsilon}{q}}$, $(\alpha > 0)$ for the low-energy side.

[1] Usually used in referring to thermionic cathodes with approximately Maxwellian electron energy distributions.

For tubes which operate on the high-energy side of the EDC – the standard vidicon, for example – the signal current is given by $I_h(v) = \int_{qv}^{\infty} N_h(\epsilon)\, d\epsilon$, where v is the voltage of the target with respect to the cathode. By substituting the approximation for $N_h(\epsilon)$ into the integral and performing the integration, we obtain $I_h(v) \approx I_{ho}\, e^{\alpha v}$, or $\frac{1}{I_h}\frac{dI_h}{dv} \approx \alpha$, $(\alpha < 0)$, making the contrast enhancement proportional to $|\alpha| = -\alpha$. For tubes which operate on the low-energy side of the EDC – the mirror tube, for example – the signal is given by $I_\ell(v) = \int_{o}^{qv} N_\ell(\epsilon)\, d\epsilon$ giving, by a similar procedure, $I_\ell(v) \approx I_{\ell o}\, e^{\alpha v}$, $(\alpha > 0)$. In this case, the contrast enhancement is proportional to α. Consequently, over the range where the exponential approximations to the high- and low-energy sides of the EDC are valid, α is a good parameter to use in comparing the effect of an electron source on a tube's contrast enhancement. The terms "high-energy cutoff" and "low-energy cutoff" will be used throughout this report when referring to the shapes of the high- and low-energy sides respectively of the EDC's of various electron sources, and these sources will be compared by the parameter α.[2]

(Recall that there are many other limitations on improving contrast, so improving α beyond about $\pm$ 100/V cannot be used to any advantage in a practical device; just utilizing the capability of a source with $\alpha = \pm$ 100/V would require considerable effort.)

As mentioned previously, not only is the electron-energy distribution important but also the spatial distribution of electrons emitted from a source. In Section II, the apparatus which was set up to determine both of these parameters is discussed. In the following sections, the two ways to improve α are presented. The use of filtering techniques to discard unwanted electrons from the energy distribution is discussed in Section III. Another approach, developing electron emitters with the desired distribution, is discussed in Section IV. Section V gives a few conclusions that resulted from this study. A Bibliography of useful references dealing with subjects found in this report is included following Section V.

---

[2] As a point of comparison, a 50-meV (FWHM) Gaussian EDC has an average α of about 70/V if $N_\ell(\epsilon)$ is approximated over the energy range containing from 4 to 40% of the total current or -70/V if $N_h(\epsilon)$ is approximated over the range containing 4 to 40% of the total current.

II. THE ANGULAR ELECTRON ENERGY ANALYZER SYSTEM

The angular electron energy analyzer (AEEA) system was built by Advanced Research Instrument Systems, Inc. (ARIS), of Austin, Texas, under Contract DAAK02-72-C-0104. It consisted of two large chambers separated by a 6-inch, metal-sealed gate valve (Figure 2). Each chamber had its own 150-ℓ/sec ion pump and titanium sublimator with cold shield, and controllers were provided to operate all of these independently. The entire system was bakeable to 300° C by enclosing it in a temperature-controlled shroud that could be lowered over it. A gas-handling system with precision leak valves was added to allow desired gases to be entered into either chamber. The pressures in the chambers were monitored by Bayard-Alpert type nude ion gauges.

The smaller chamber, the cathode preparation chamber (CPC), contained an array of four evaporator ovens, a cesium source, and a silver oxygen leak. These could be used to fabricate or activate samples while the gate valve was closed and thus prevent contamination of the electron energy analyzer in the other chamber. The CPC also contained numerous accessory flanges. Mounted on these were windows for sample observation or illumination and mechanical and electrical feedthroughs for electron-emission monitoring and cathode processing. An EAI Quad 250B residual gas analyzer was used to monitor the gases present during cathode processing. The sample could also be moved by a manipulator from the CPC out through the top flange. Here, it could be RF heated and sealed into its own vacuum tube or returned to the main chambers for further processing or evaluation. This top port also served as the primary place for samples to be entered into or removed from the system.

Various sample holders were fabricated, each to accommodate a particular type of electron emitter. A sample holder could be connected to as many as eight electrically isolated leads on the manipulator. This allowed multiple-sample testing without cycling the vacuum system back to air. (This was particularly useful in investigating the field-emitter tips because each pumpdown also required an extensive bake-out.) In either chamber, the sample holder could also be cooled to about 100° K by liquid nitrogen.

The larger chamber contained the electron energy analyzer (EEA). The analyzer rested on a carriage which could be pivoted ± 90° horizontally about the sample position. This made measurement of the polar, θ, angular dependence quite simple. However, since the sample could not be rotated while in position for EDC measurements, it was difficult to measure the azimuthal, ϕ, angular dependence. To change ϕ, the sample holder had to be removed from the system and rotated on its support rod. (Systems have been designed to measure both θ and ϕ; for an example, see the article

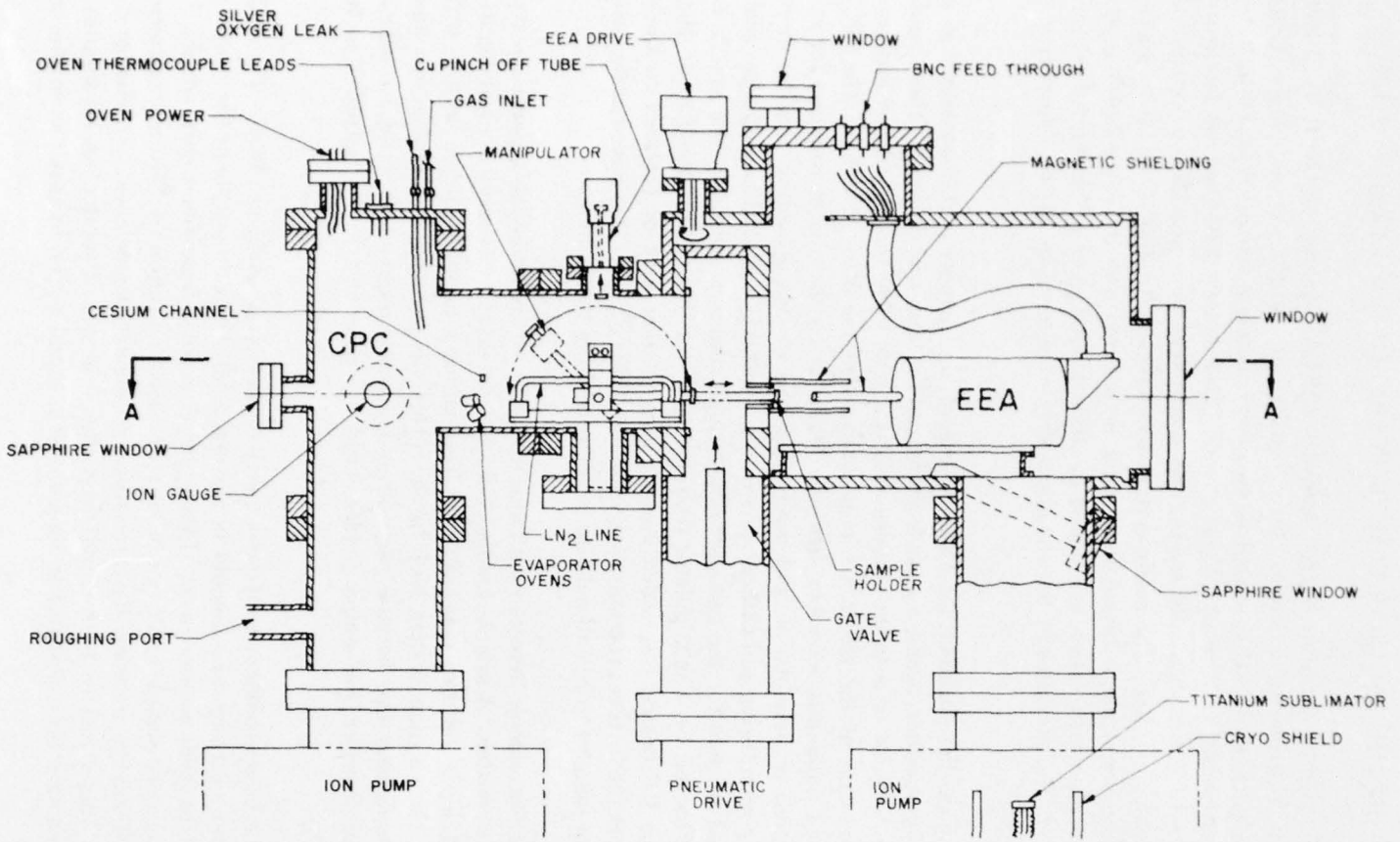

Figure 2A. The Angular Electron Energy Analyzer (AEEA) system used to activate and evaluate electron emitter samples.

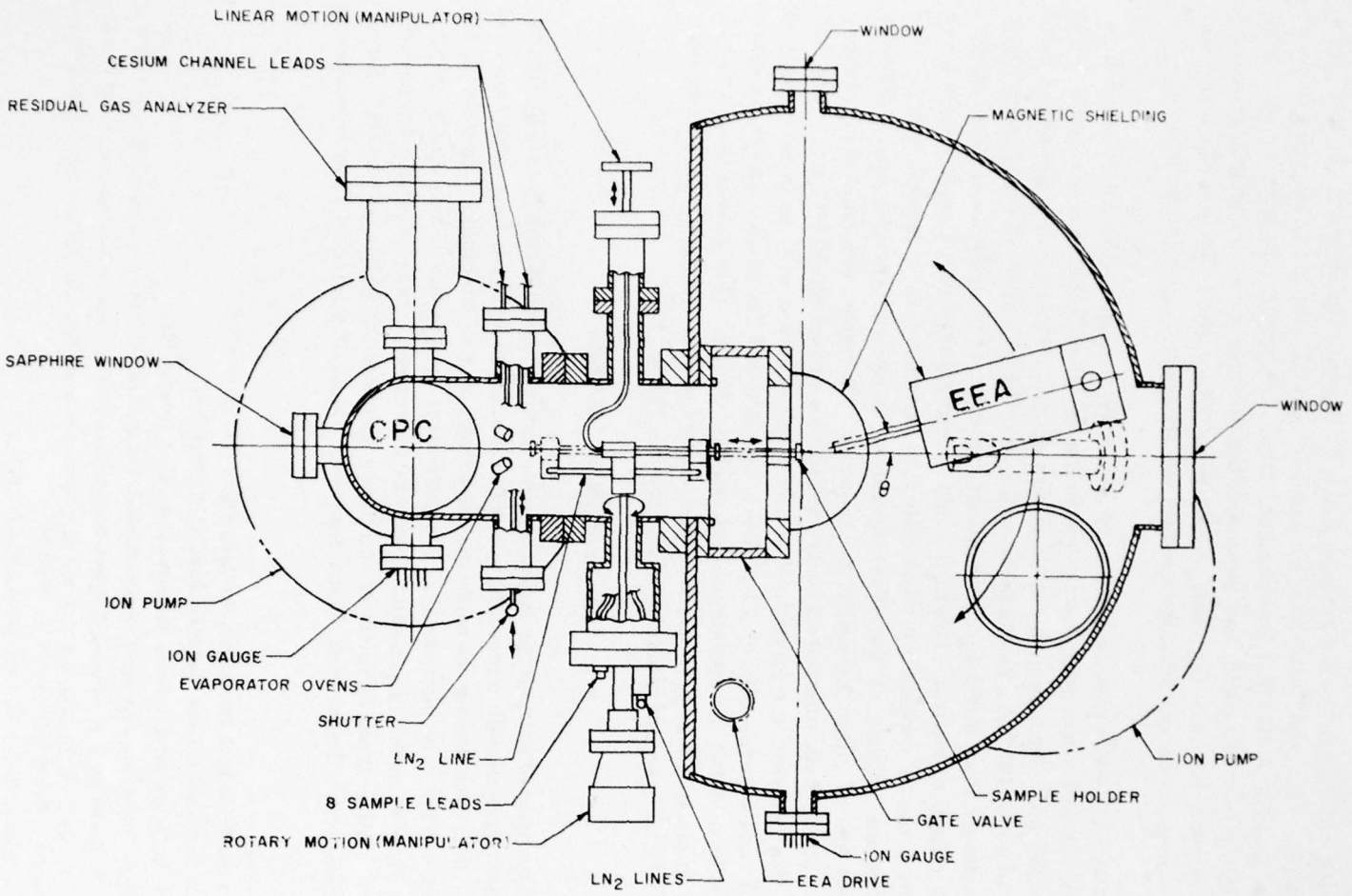

SECTION A-A

Figure 2B. The AEEA (Section A-A of Figure 2A).

by Smith and Traum.[3]) The analyzer had a 1° aperture for accepting electrons from the sample. This could have been increased to about 5°, the limitation being imposed by the opening in the first lens element. (Had the aperture size been increased, the collection efficiency would have improved; but not only would the angular resolution have dropped but also the energy resolution. Since the collection efficiency was always adequate for our tests, the aperture was always set to give 1° resolution.)

The EEA was a retarding potential difference analyzer – the ARIS model EEA-2100A. It had a maximum-energy resolution of 30 meV but was adjustable up to about 250 meV depending on the sensitivity desired. It had an ultimate current sensitivity of about 10^{-14} A. The analyzer could sweep up to a 50-eV electron energy range automatically from 0.005 to 2.5 eV/sec or could be set manually to monitor any particular energy of interest. The EDC could be plotted directly on an X-Y recorder or displayed on an oscilloscope from either an automatic or a manual sweep. The analyzer was capable of the above operation at electron energies up to 2000 eV without loss of either sensitivity or resolution. Of course, one must always make a choice in the trade-offs among energy resolution, current sensitivity, and sweep rate. With this analyzer, a resolution of 50 meV was observed with an input current of 10^{-9} A and a sweep rate of 25 meV/sec. Golden and Zecca have written an article describing in detail the operation of this analyzer design.[4] (For a discussion of various types of electron energy analyzers and the effect of their geometry on their measurement of EDC's, see the article by Di Stefano and Pierce.[5])

III. ELECTRON FILTERS

One way to sharpen the cutoffs in the electron energy distribution is by filtering out the electrons with undesirable energies. Numerous methods have been employed to do this, each having its particular advantages and disadvantages. In general, the techniques are very inefficient, i.e., to increase α by a factor of two usually requires more than an order of magnitude decrease in current. Four general references discussing various types of filters or comparing their characteristics are Septier,[6] Kuyatt and Simpson,[7] Hafner *et al.*,[8] and Simpson.[9] Most of the recent filter development

---

3 N. V. Smith and M. M. Traum, *Phys. Rev. Lett.*, 31, 20, 1247 (12 Nov 73).

4 D. E. Golden and A. Zecca, *Rev. of Sci. Instr.*, 42, 2, 210 (Feb 71).

5 T. H. Di Stefano and D. T. Pierce, *Rev. of Sci. Instr.*, 41, 2, 180 (Feb 70).

6 Albert Septier, ed., *Focusing of Charged Particles*, Vol. 2, Chap. IV, "Prisms" (Academic Press, N.Y., 1967).

7 C. E. Kuyatt and J. A. Simpson, "Electron Monochrometer Design," *Rev. of Sci. Instr.*, 38, 1, 103 (Jan 67).

8 H. Hafner, J. A. Simpson, and C. E. Kuyatt, "Comparison of the Spherical Deflector and Cylindrical Mirror Analyzers," *Rev. of Sci. Instr.*, 39, 1, 33 (Jan 68).

9 J. A. Simpson, *Rev. of Sci. Instr.*, 32, 12, 1283 (Dec 61).

has resulted from the work on electron spectroscopy, but this has relied heavily on the earlier work on mass spectrometers. The filters are generally one of two types – electrostatic or magnetic – although there are some filters that use a combination of both types of fields. Most filters use steady state fields, but there are techniques that employ fluctuating fields. Some of the common types of electrostatic filters are the parallel plate,[10] [11] the retarding potential,[12] the spherical,[13] the cylindrical mirror,[14] [15] the multipole (especially, the quadrupole),[16] [17] the 127° cylindrical,[18] [19] and the monokinetron.[20] [21] In addition, simple electron lenses can be used to some degree for electrostatic filtering since their focal lengths depend on electron energy. Three types of electrodynamic filters are the time of flight filter,[22] the retarding potential difference analyzer (actually a quasi filter),[23] and the electron buncher.[24]

Although most work was done on magnetic filters in the early days of electron spectroscopy, their size, weight, power requirements, and always present stray magnetic fields have relegated them to a position of secondary importance for most applications. Nevertheless, some of the more noteworthy designs employing magnetic fields are the homogeneous magnetic field with radial electric field,[25] the double-focusing spectrograph,[26] the trochiodal monochromator,[27] and the wien filter.[28] [29]

---

[10] G. A. Harrower, *Rev. of Sci. Instr.*, 26, 9, 850 (Sep 55).

[11] T. S. Green and G. A. Proca, *Rev. of Sci. Instr.*, 41, 10, 1409 (Oct 70).

[12] J. A. Simpson, *Rev. of Sci. Instr.*, 32, 12, 1283 (Dec 61).

[13] E. M. Purcell, *Phys. Rev.*, 54, 10, 818 (15 Nov 38).

[14] S. Aksela, *Rev. of Sci. Instr.*, 42, 6, 810 (Jun 71).

[15] J. S. Risley, *Rev. of Sci. Instr.*, 43, 1, 95 (Jan 72).

[16] Conrad Schmidt, *Rev. of Sci. Instr.*, 41, 1, 117 (Jan 70).

[17] A. E. Holme, *et al.*, *Vacuum*, 24, 1, 7 (Oct 73).

[18] M. Arnow and D. R. Jones, *Rev. of Sci. Instr.*, 43, 1, 72 (Jan 72).

[19] J. J. Leventhal and G. R. North, *Rev. of Sci. Instr.*, 42, 1 (Jan 71).

[20] Paul Marmet, *Rev. of Sci. Instr.*, 39, 12, 1932 (Dec 68).

[21] D. Roy and J. D. Carette, *Rev. of Sci. Instr.*, 42, 6, 776 (Jun 71).

[22] G. C. Baldwin and S. I. Friedman, *Rev. of Sci. Instr.*, 38, 4, 519 (Apr 67).

[23] R. E. Fox, *et al.*, *Rev. of Sci. Instr.*, 23, 12, 1101 (Dec 55).

[24] A. D. Sushkov, Russian Pat. No. 247427 (available from DDC-AD No. 743664).

[25] J. Mattauch and R. Herzog, *Zeits.f. Physik*, 89, 786 (1934).

[26] J. Mattauch, *Phys. Rev.*, 50, 7, 617 (1 Oct 36).

[27] D. Roy, *Rev. of Sci. Instr.*, 43, 3, 535 (Mar 72).

[28] H. Boersch, *Zeits. f. Physik*, 139, 115-46 (1954).

[29] W. H. J. Anderson, *Br. J. Appl. Phys.*, 18, 1573-9 (1967).

Two electron sources using filtering techniques were fabricated under this work unit. A 127° cylindrical electron monochromator was built in-house, and a 180° spherical filter was built under an external contract. Both used electrostatic filtering of electrons from interchangeable, thermionic cathodes. (These commercially available cathodes were oxide coated with indirect heaters.) These sources were designed to investigate far infrared sensing layers for direct-view tubes.

A. The 127° Cylindrical Filter

An electron source using a 127° electrostatic filter was fabricated in-house (Figure 3). Electrons from the gun were focused into the entrance aperture of the filter. Once inside, the electrons were deflected by the electric field between the cylindrical plates. Those of a particular energy were focused into the output slot and escaped while all others were collected by the plates. (This focusing property at 127° was first shown by Hughes and Rojansky.[30])

The walls of the cylindrical plates were coated with amorphous carbon by electron beam evaporation from a carbon block. This was done for two reasons. First, carbon has a very uniform work function, and, as a result, the potential variations near carbon-coated surfaces have a minimum effect on low-energy electrons passing near them. Second, carbon is an effective absorber of infrared radiation. Since the thermionic cathode radiated a large amount of infrared energy, the more energy that could be absorbed in the filter, the less that was transmitted to interfere with the infrared sensor measurements near the output from the slot.

A novel feature of this filter was the use of conductive films to correct for the fringing fields at both the top and bottom of the cylindrical plates and at the entrance aperture and exit slot. Once again, amorphous carbon was the choice for the reasons already stated. The carbon was deposited on glass pieces cut to fit as shown in Figure 3. (For a review of the use of carbon in high vacuum work, see the article by Beitel.[31])

This source was operated only briefly; consequently, its capability was never fully investigated. It was superseded by the electron source described in Section B.

B. The Hemispherical Filter

An electron source was fabricated by ARIS under Contract DAAK02-71-C-0540. Details of the electron optics of this device are shown in Figure 4. In this source,

---

30 A. L. Hughes and V. Rojansky, *Phys. Rev.*, 34, 2, 284 (15 Jul 29).

31 G. A. Beitel, *J. of Vac. Sci. & Tech.*, 8, 5, 647 (1971).

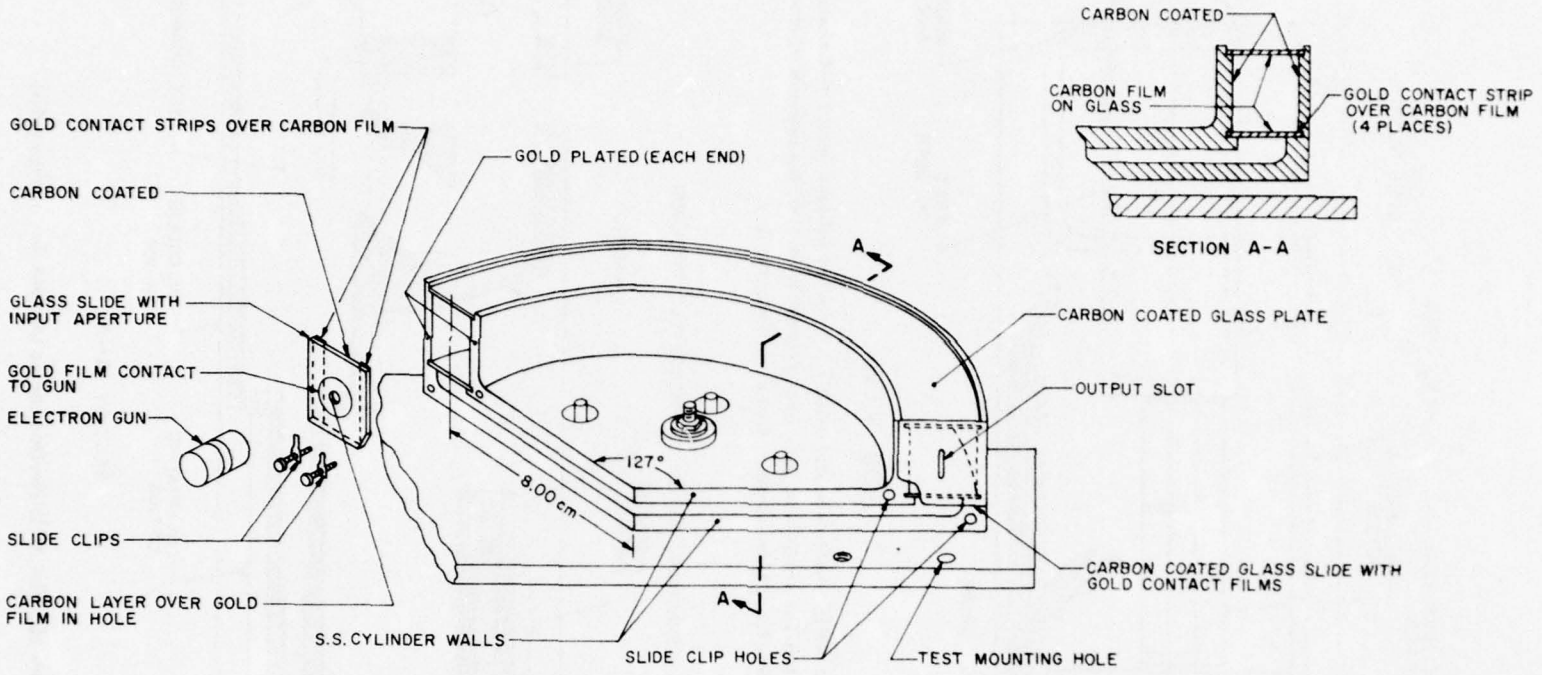

Figure 3. The electron source using a 127° cylindrical electrostatic filter. Fringing fields were avoided by the use of carbon films.

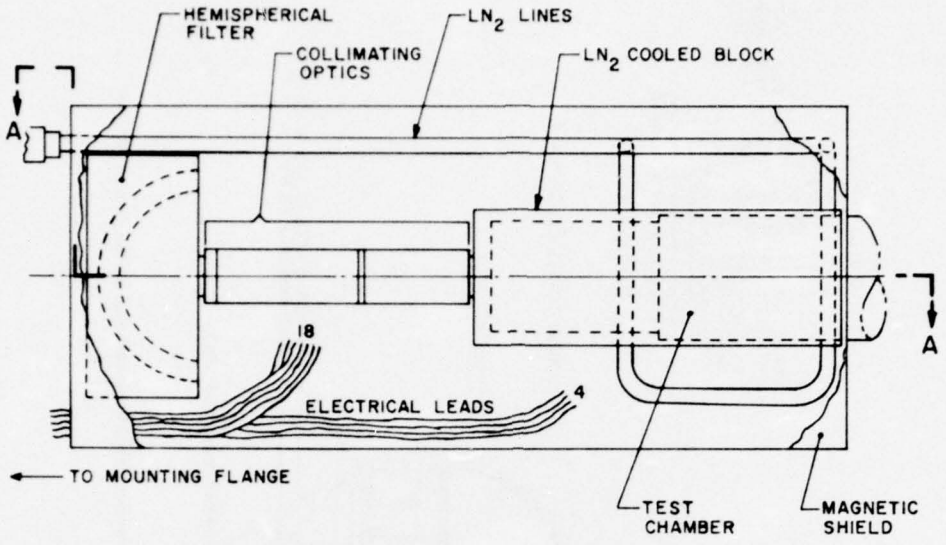

SIDE VIEW

Figure 4A. The ARIS electron source with LN_2 cooled infrared sensor test chamber. The electrons from the thermionic gun were filtered by a 180° hemispherical, electrostatic filter and flooded a 1-cm-diameter area in the test chamber.

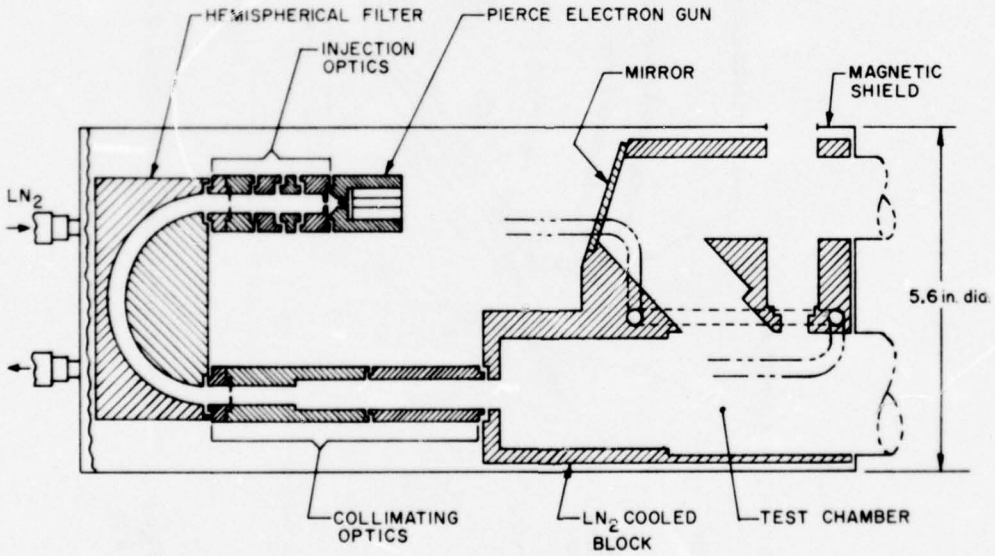

SECTION A–A

Figure 4B. The ARIS electron source (section A-A of Figure 4A).

electrons from a thermionic cathode were directed into a 180° hemispherical, electrostatic filter.[32] Lenses following the filter projected a 1-centimeter-diameter flood beam into a liquid nitrogen cooled block. The block's test chamber could accommodate many different detector configurations since there were several electrical leads into it. (One lead was a high-voltage lead for a phosphor.) This electron source could be used to test an infrared-sensitive retina in either the transmission or reflection mode.

The energy distribution of this source was checked with the AEEA at current levels below 10^{-9} A and found to be nearly Gaussian with a 43-meV (FWHM) energy spread. This gave useful α's of better than -80/V for the high-energy cutoff and of about 60/V for the low-energy cutoff.[33] In tests at higher current levels, the high-energy cutoff was measured with a field-shielded retarding grid in the test chamber. For the transmitted current range, 8×10^{-9} A to 8×10^{-8} A, α averaged -55/V, while for the range, 4×10^{-8} A to 4×10^{-7} A, α averaged only -30/V.

The uniformity of the flood beam was checked by placing a high-voltage phosphor behind the retarding grids in the test chamber. (An additional shield grid was placed between the retarding grid and the phosphor to prevent field distortion near the retarding grid.) Although the source was designed to provide a spot uniformity of 5%, the phosphor showed that about 20% was the lowest achievable at α's better than -20/V. This seriously limited the usefulness of this source.

IV. ELECTRON EMITTERS

In the previous section, filtering methods of sharpening the cutoffs in the electron energy distribution curve (EDC) were cited. It should be obvious to the reader that those methods have many disadvantages for tube applications. If a reliable electron emitter could be fabricated with the desired EDC as well as with other required characteristics, then the filter would not be needed and the complexities associated with adding it could be avoided. In this section, several electron emitters are discussed; but, at the present time, none are sufficiently developed to replace the thermionic cathode on a large scale.

From the first days of the electron tube, the hot thermionic cathode has been the major electron source. Its normal EDC, $N(\epsilon)$, can be approximated very accurately by the high-energy tail of the classical Boltzmann distribution of energies:

---

[32] For a description of the theory of focusing by use of this filter, see E. M. Purcell, *Phys. Rev.*, 54, 10, 818 (15 Nov 38).

[33] Although the Gaussian EDC is symmetrical about the most probable energy and $\alpha_\ell = -\alpha_h > 80$/V for symmetrical energy ranges, the useful α_ℓ does not equal the useful α_h because they must be determined by approximating over unsymmetrical energy ranges.

$$N(\epsilon) = \begin{cases} A \exp \dfrac{\Phi - \epsilon}{kT} & \epsilon > \Phi \\ 0 & \epsilon < \Phi \end{cases}$$

where A is just a proportionality constant; ϵ, the normal energy of an electron (the total energy E minus the energy ϵ_o due to the velocity parallel to the surface, i.e., $\epsilon = E - \epsilon_o$); Φ, the work function of the emitter surface; k, Boltzmann's constant; and T, the absolute temperature (Figure 5a). This gives a sharp, low-energy cutoff which is limited only by practical electron optics design in the tube. Although this is good for mirror tube operation, most image tubes require a sharp, high-energy cutoff. For the high-energy cutoff, $\alpha = -\dfrac{1}{kT}$. Since the temperature must be high ($> 800°$ C) in order to give sufficient energy to overcome the work-function barrier to enough electrons to provide useful current levels, an α of about -14/V is the best obtainable high-energy cutoff with low-work-function coatings on thermionic cathodes. Well designed electron guns using thermionic cathodes rarely achieve better than -10/V. (Recent improvements in thermionic cathodes have been the development of the LaB_6 emitter surface[34] and the thorium carbide cathode.[35])

Figure 5b shows the total energy distribution of electrons from a thermionic cathode. Notice that these cutoffs are not as sharp as those of the normal EDC. Unfortunately, any application where electron optics are used to collimate or focus the electron beam employs more nearly the total EDC unless filtering techniques are employed.

In the thermionic cathode, it is the high temperature that limits its usefulness. High temperature plays a similar role in all types of electron emitters; therefore, only cold cathode schemes were investigated under this work unit. A large amount of work has already been done in the last decade on various cold cathodes. Some of the approaches are field emission,[36 – 41]

---

[34] M. Nasimi, *Rev. of Sci. Instr.*, 42, 12, 1765 (Dec 71).

[35] H. H. Glascock, *Rev. of Sci. Instr.*, 43, 4, 698 (Apr 72).

[36] R. N. Thomas, *et al.*, "Fabrication and Application of Large Area Silicon Field Emitter Arrays," *Sol. State Electronics*, 17, 2, 155 (Feb 74).

[37] C. A. Spindt, "Thin Film Field Emission Devices," IEEE Conference on Elec. Device Tech., N.Y. (1973).

[38] Lea Colin, *J. Phys. D: Appl. Phys.*, "Field Emission from Carbon Fibers," 6, 1105 (1973).

[39] W. D. McNeil and W. B. Shepard, "Preparation of Ge and Si Field Emission Cathodes," *Rev. of Sci. Instr.*, 43, 11, 1636 (Nov 72).

[40] J. D. Levine, "Analysis and Optimization of a Field Emitter Array," *RCA Review*, 32, 1, 144 (Mar 71).

[41] Joe Shelton [Oxide Metal Composite for] "Field Effect Emission," Report RN-TR-71-1, Redstone Arsenal, Alabama (Aug 71), (available from DDC).

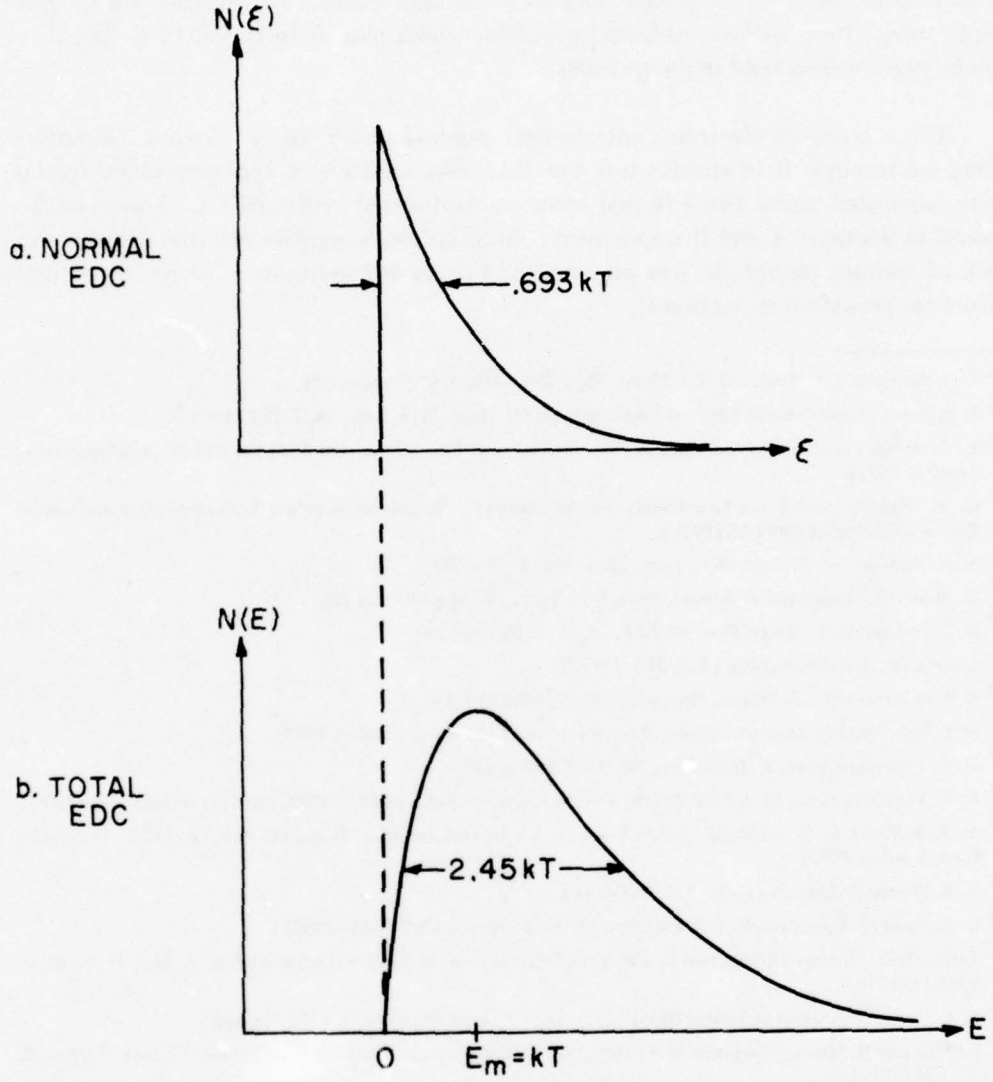

Figure 5. Thermonionic energy distribution curves (EDC's) of all electrons emitted into 2π *steradians about the surface* normal for: (a) the normal component of each electron's energy, ϵ, and (b) the total energy of each electron, E. The most probable total energy $E_m \approx 26$ meV at room temperature.

emission from p-n junctions,[42-47] NEA photoelectric emission,[48-51] secondary electron emission,[52-54] emission from Schottky surface barrier diodes,[55-57] and thin film tunnel emission.[58-64] Although some of these approaches are being used for specific applications, they all have technical problems which remain to be solved before they can be more widely used in image tubes.

Three types of electron emitters were studied under this work unit. Emitters using microscopic field emitter tips and thin film emitters of heat-treated tin oxides were fabricated under two external contracts and tested in the AEEA. These are discussed in Sections A and B respectively. In addition, a negative electron affinity surface of gallium phosphide was prepared and evaluated in-house. The results of that effort are presented in Section C.

---

42 D. J. Bartelink, J. L. Moll, and N. I. Meyer, *Phys. Rev.*, 130, 3, 972 (1 May 63).

43 E. S. Kohn, "Cold Cathode Electron Emission from Si," *Appl. Phys. Lett.*, 18, 7, 272 (Apr 71).

44 P. J. Deasley and K. R. Faulkner, in *Adv. in Elec. and Elec. Phys.*, Vol 33A, pp. 459-67 (Academic Press, London, 1972).

45 D. E. Bolger, "GaAsP for Low Energy Spread Cathodes," Report by Standard Telecommunications Lab on British CVD Project #RP7-68 (1971).

46 K. R. Faulkner, *et al.*, *Appl. Phys. Lett.*, 23, 6, 298 (15 Sep 73).

47 H. Shade, H. Nelson, and H. Kressel, *Appl. Phys. Lett.*, 20, 10, 385 (May 72).

48 R. L. Bell and W. E. Spicer, *Proc. of IEEE*, 58, 11, 1788 (Nov 70).

49 J. van Laar, *Acta Electronica*, 16, 3, 215 (Jul 73).

50 B. F. Williams and J. J. Tietjen, *Proc. of IEEE*, 59, 1489 (1971).

51 R. L. Bell, *Negative Electron Affinity Devices* (Oxford Univ. Press, London, 1973).

52 M. K. Testerman, *et al.*, *J. Appl. Phys.*, 36, 9, 2939 (Sep 65).

53 R. U. Martinelli, *et al.*, RCA Final Report on USA Contract DAAK02-71-C-0329 (Sep 72) (available from DDC).

54 B. F. Williams, R. U. Martinelli, and E. Kohn, in *Adv. in Elec. and Elec. Phys.*, Vol 33A, pp. 447-57 (Academic Press, London 1972).

55 R. K. Swank, *J. Appl. Phys.*, 41, 2, 778 (Feb 70).

56 C. A. Stolte, J. Vilms, and R. J. Archer, *Sol. State Electronics*, 12, 945-54 (1969).

57 Tohru Itoh, "Energy Distribution of Electrons Emitted from Si Surface Barrier Diodes," *J. Appl. Phys.*, 41, 5, 1951 (Apr 70).

58 C. A. Mead, "Operation of Tunnel Emission Devices," *J. Appl. Phys.*, 32, 4, 646 (Apr 61).

59 J. May and R. Hrach, "Emission of Electrons from MIM Systems: Angular Distributions," *Czech. J. Phys. B*, 23, 234 (1973).

60 R. Hrach, "Emission of Electrons from MIM Structures: Discussion of Processes in the Cathode," *Czech. J. Phys. B.*, 23, 225 (1973).

61 R. Hrach ". . . Emission from MIM System: Energy Distributions," *Czech. J. Phys. B.*, 18, 12, 1591 (Dec 68).

62 J. Schröfel and I. Hüttel, *Thin Solid Films*, 21, 53 (1974).

63 C. A. Taheri, *et al.*, "Electrical Forming in and Electron Emission from Thin Film Aluminum-Borosilicate Glass-Aluminum Sandwiches," *Phys. Stat. Sol.*, A12, 2, 563 (1972).

64 H. Biederman, "Electron Emission into Vacuum from Al-LiF-Au Structures," *Thin Solid Films*, 18, 1, 39 (1973).

A. Miniature Field-Emitter Tips

The advantage of using field emitters to improve the contrast enhancement in some tubes is shown by the sharp, high-energy cutoffs of the EDC's in Figure 6. The expression for the total energy distribution, N(E), is

$$N(E) = \frac{J_o}{d} \frac{\exp \frac{E}{d}}{1 + \exp \frac{E}{kT}}$$

where E is the total energy of an emitted electron, J_o, the total emitted current density, and d, a factor determined primarily by the work function. At low temperatures ($kT \ll d$), the $\exp \frac{E}{kT}$ term dominates the expression at high electron energies ($E > kT$). This causes the high-energy cutoff to be very sharp, i.e., $\alpha \simeq - \frac{1}{kT}$. At 77° K, $\alpha \simeq -145/V$; but, even at room temperature, $\alpha \simeq -25/V$. The low-energy cutoff is not nearly as sharp. Notice that it does not vary with temperature but depends only on the value of d. Typical values of d give an α of only about 6.5/V. (These results were first demonstrated experimentally by Muller and Young[65] [66] in 1959. Experimental and theoretical work on field emission was recently reviewed by Gadzuk and Plummer.[67] Their article contains an extensive bibliography of the previous work in this field.)

The field-emitter tips investigated under this work unit were prepared by Stanford Research Institute (SRI) under Contract DAAK02-72-C-0144.[68] Twenty samples were fabricated, each with eight independent emitter tips. Figure 7 shows the physical configuration of a sample. The tips were fabricated by depositing 1-μm cones in small holes etched in the dielectric film. A voltage of about 100 V on the anode was sufficient to emit about 10^{-9} A from a single tip.

Although many of the SRI samples were run in the AEEA, an EDC measurement was never attempted on any of these tips because their electron-emission currents were so erratic. SRI found that a 350° C bakeout in a vacuum of 10^{-9} Torr for 100 hours reduced the noise in the emission current to about 1% for about 6 hours. However, this high-temperature bakeout was not duplicated in the AEEA. Nevertheless, a 1.5-nA

---

[65] R. D. Young, "Theoretical Total Energy Distribution of Field Emitted Electrons," *Phys. Rev.*, 113, 1, 110 (1 Jan 59).

[66] R. D. Young and E. W. Muller, "Experimental Measurement of Total Energy Distributions of Field Emitted Electrons," *Phys. Rev.*, 113, 1, 115 (1 Jan 59).

[67] J. W. Gadzuk and E. W. Plummer, "Field Emission Energy Distributions," *Rev. of Modern Phys.*, 45, 3, 487 (Jul 73).

[68] C. A. Spindt, "Low Energy Monoenergetic Flood Source," Final Report of USA Contract DAAK02-72-C-0144 (Sep 72) (available from DDC).

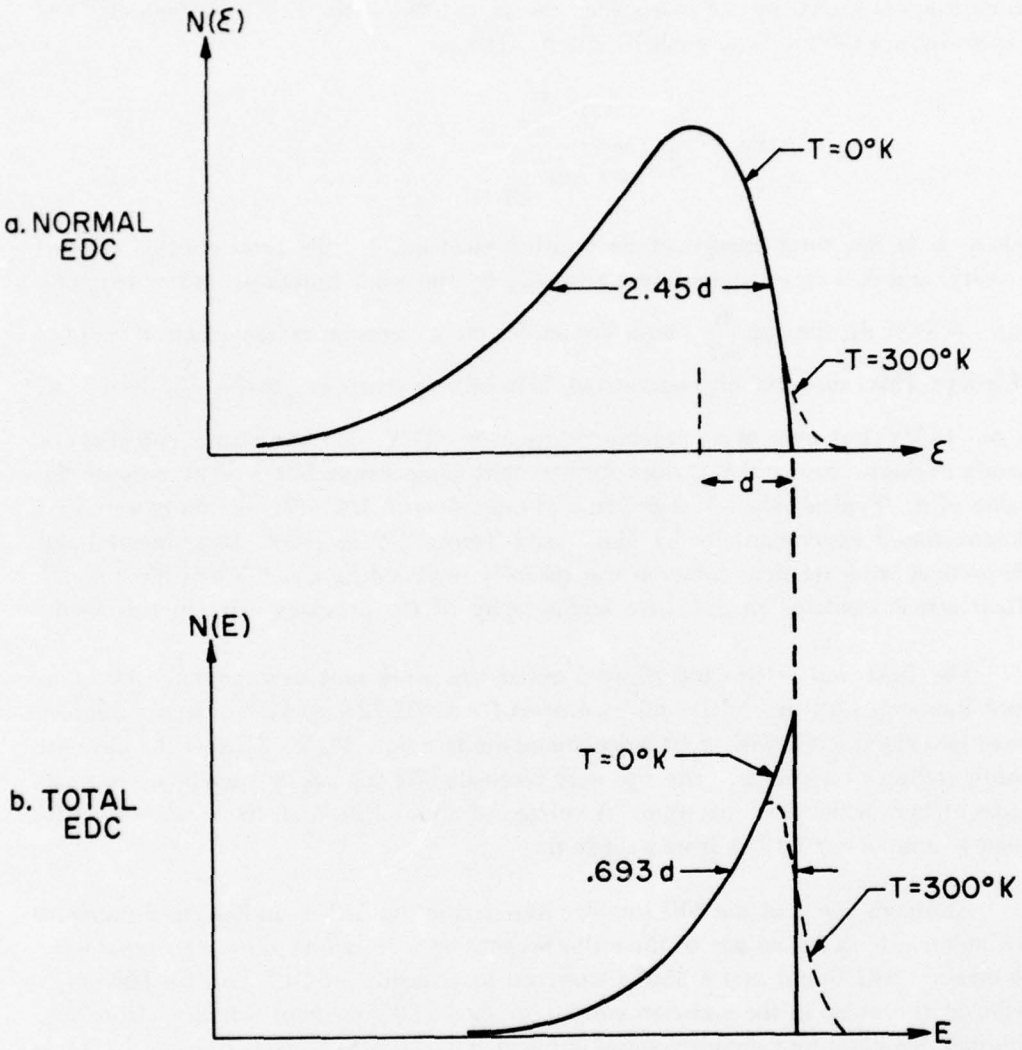

Figure 6. Field emission energy distribution curves of all electrons emitted into 2π steradians about the surface normal for: (a) the normal component of each electron's energy, ϵ, and (b) the total energy of each electron, E. The parameter, d, is determined from the work function. (Notice the mirror symmetry with Figure 5.)

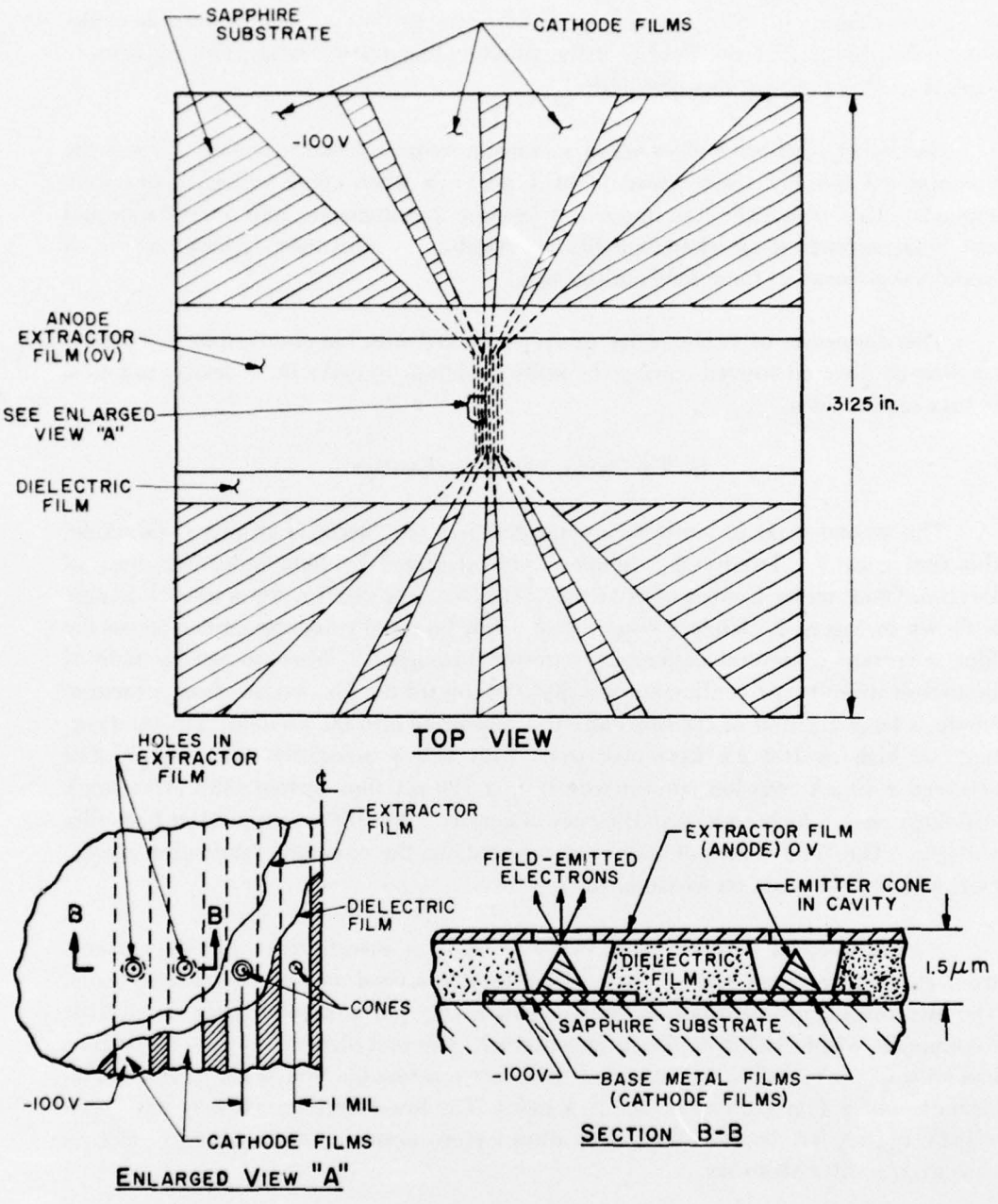

Figure 7. Miniature field emitter structure fabricated by Stanford Research Institute. Enlarged View "A" shows four of the eight addressable electron emitter cones with portions of the overlayers removed to expose the underlying structure.

current, stable for 20 min, was achieved after an extensive 250° C bakeout. Most of this current appeared to be directed within 5° of the surface normal. A possible explanation for this is that the field near the anode collimates the beam, but much more work is needed to verify this speculation.

One other significant observation was made on one of these samples. Two of the tips emitted initially stable currents of 1 nA each when equal voltage biases were applied. This observation is important because simultaneous turn-on voltages and matching current-voltage characteristics are required in most tube applications which would use an array of these field-emitter tips.

This discussion of field-emitter tips is concluded with the observation that efforts need to be directed toward solving the noise problems to make these devices practical in tube applications.

B. Tin Oxide, Thin-Film Emitter

The second type of emitters investigated was the "variable affinity," tin oxide, thin-film emitter. Twenty-one samples were fabricated by Beta Industries, Inc., of Dayton, Ohio, under Contract DAAK02-72-C-0163. The configuration of each sample is shown in Figure 8. When a potential of a few hundred volts was applied across the film, a current of several milliamperes flowed through it. When an electric field of thousands of volts per centimeter was directed toward the film surface from a vacuum anode, a large fraction of the film current was emitted into the vacuum. Emission currents as high as 100 μA were observed. With 440 V across the film, sample #12 achieved a 40 μA emission current with only a 120 μA film current (33% efficiency). Although such a high emission efficiency was rare, 5 to 10% was typical at high film voltages. The final report of that contract contains the complete fabrication parameters and emission data on all samples.[69]

Several samples were mounted in the AEEA for investigation, but the currents from all of them were rather noisy. Despite this, several measurements were made. The electron energy distribution and current density per unit solid angle varied little for emission within 15° from the surface normal. The best high-energy cutoff observed had an α of -5/V. (This was observed with 130 V across the film, 6 μA total emission current, and a film current of about 1 mA.) The low-energy cutoff may have been slightly better, but because there was always more noise in the low-energy electron current, it is difficult to say.

---

[69] J. L. Mize, "Investigation of Solid State Cold Cathodes," Final Report on USA Contract DAAK02-72-C-0163 (Jun 72) (available from DDC).

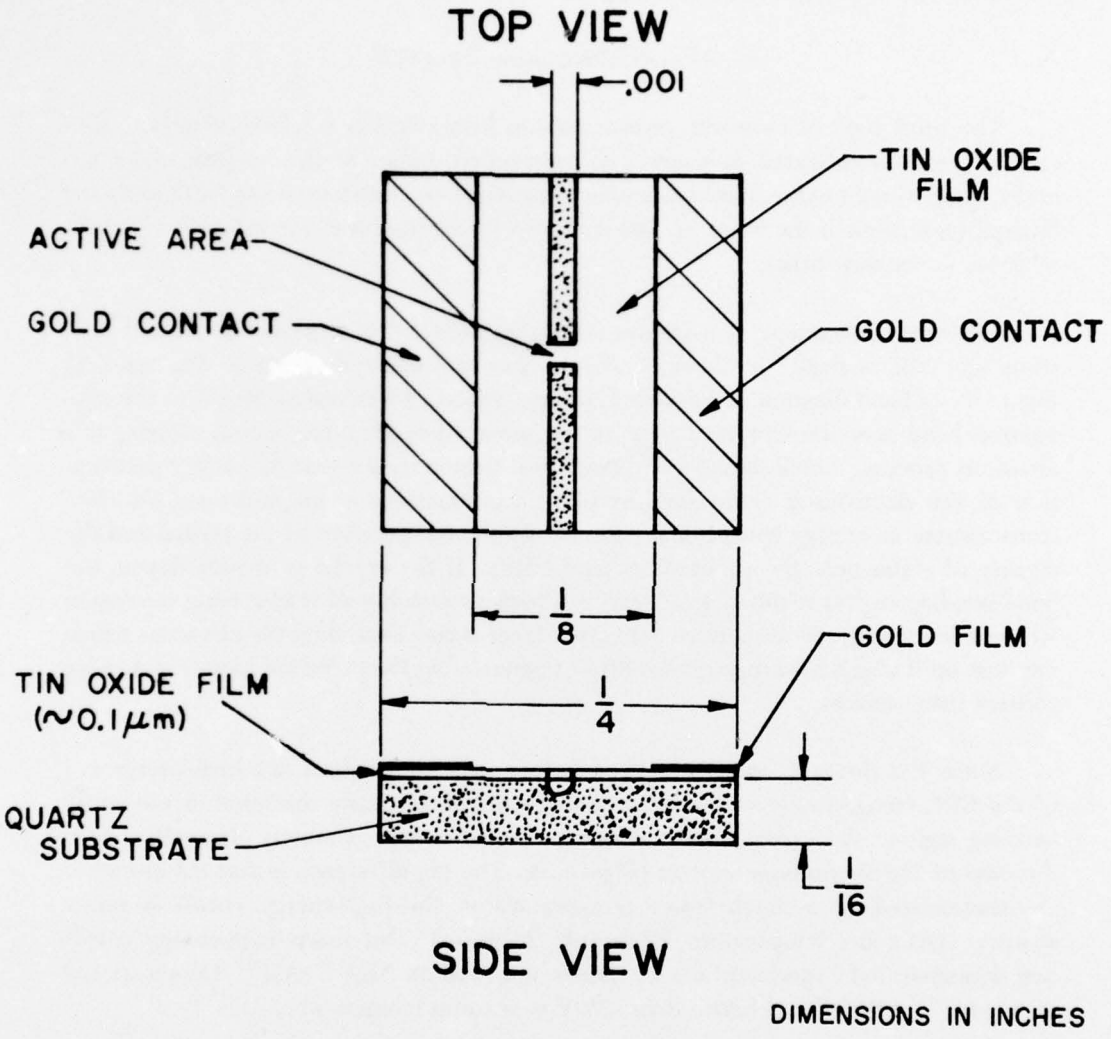

Figure 8. The tin oxide, thin-film emitter fabricated by Beta Industries. The active area (area where large voltage drop occurred) was confined to the center by removal of a portion of the tin oxide film with a diamond scribe. (See top view.)

An accurate model for emission from these devices has not yet been formulated. Mize[70, 71] has hypothesized semi-cylindrically, symmetrical junctions as the active portion of the device, but electron microscope studies showed this to be an inaccurate description for emission from our samples.

C. NEA Photoemission from GaP

The third type of emission, photoemission from negative electron affinity (NEA) surfaces, was investigated in-house. As mentioned earlier in this section, there are many types of cold cathode schemes under investigation elsewhere using NEA surfaces; but photoemission is the simplest, and it looked promising for use in infrared, velocity-selector, direct-view tubes.

The major advantage of using the NEA approach is that most of the emitted electrons are "thermalized" *in the bulk before they are emitted.* This is illustrated in Figure 9 – a band diagram of a cesiated, p-type crystal. Electrons excited into the conduction band near the surface diffuse to the narrow band-bending region. During this diffusion process, the electrons are thermalized (which means that the energy distribution of the electrons is determined by photon interactions in the bulk, and the electrons assume an energy spread characterized by the temperature of the crystal and the density of states near the conduction-band edge). If the crystal is heavily doped, the band-bending region is short, and there is a high probability of transversing the region *without scattering.* If the surface-activation layer is also thin, then the electrons which impinge on it also have a high probability of penetrating the potential barrier and being emitted into vacuum.

Since the electrons are thermalized before they are emitted, the high-energy tail of the EDC consists only of electrons that are not inelastically scattered in the band-bending region. As a result, the high-energy cutoff is approximately Maxwellian as in the case of the thermionic emitter (Figure 5). The big difference is that the electrons are *thermalized at a much lower temperature* so the high-energy cutoff is much sharper. (At room temperature, kT is only 26 meV.) This sharp, high-energy cutoff was demonstrated experimentally by James and Moll on NEA GaAs.[72] They achieved α's of -60/V at 80° K and better than -20/V near room temperature.

---

[70] J. L. Mize, "Investigation of Solid State Cold Cathodes," Final Report on USA Contract DAAK02-72-C-0163 (Jun 72) (available from DDC).

[71] J. L. Mize, "Research and Fabrication of Solid State Emitter Arrays," Final Report on USA Contract DAAB02-72-C-0195 (Feb 74) (available from DDC).

[72] L. W. James and J. L. Moll, *Phys. Rev.*, 183, 3, 740 (15 Jul 69).

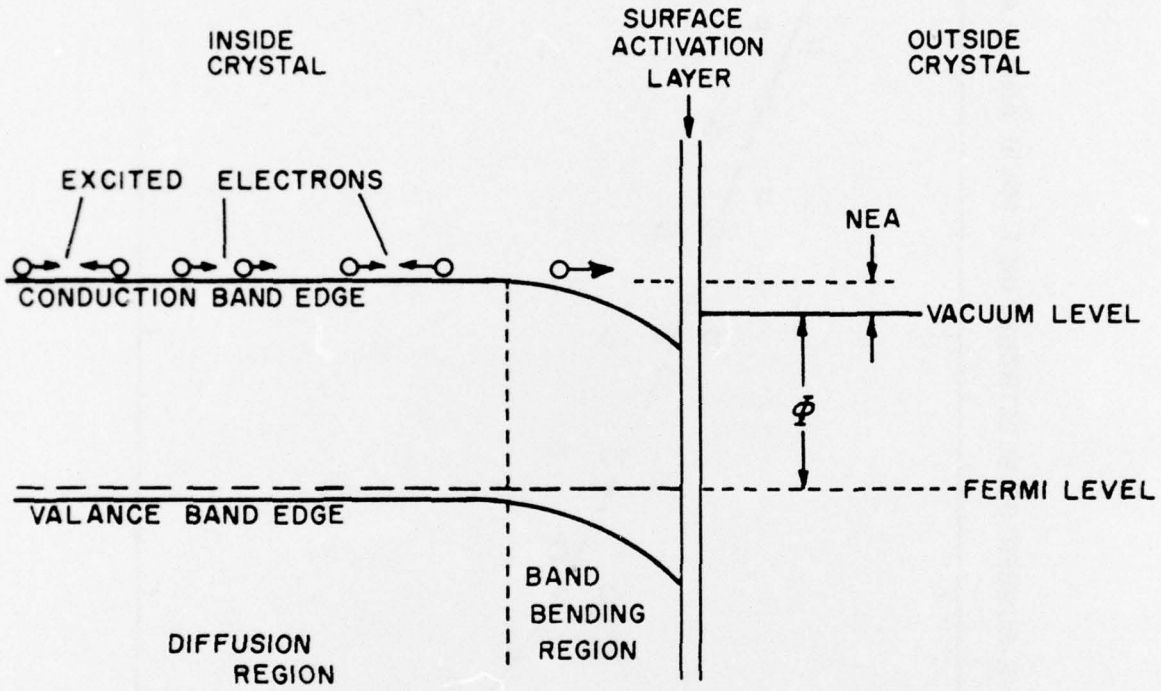

Figure 9. Electron energy diagram showing band bending near the negative electron affinity (NEA) surface of a p-type crystal. Electrons, excited to the conduction band, diffuse to the band-bending region where they are accelerated to the surface with a high probability of emission over the work-function barrier, Φ.

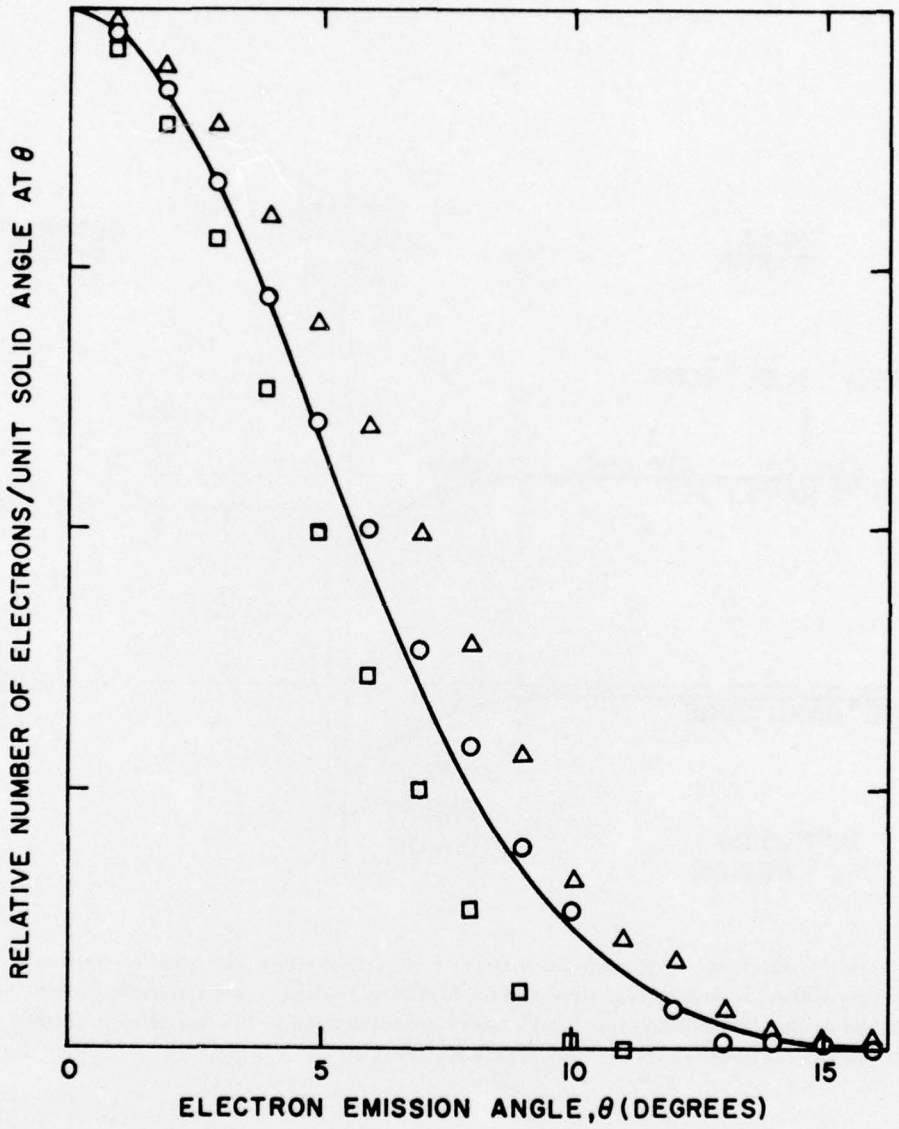

Figure 10. The distribution of emitted electrons as a function of emission angle, θ, from the (100) surface normal of a p-type GaP crystal activated to NEA by use of Cs. The data points are for three different activations. The solid line is the distribution expected from theory.

The low-energy tail is a little more complicated. If the NEA is large, then some of the electrons which are scattered in the band-bending region still have sufficient energy to escape from the surface. Consequently, the low-energy cutoff of the EDC is determined by scattering processes and is not as sharp as the low-energy cutoff of the thermionic cathode. This is not the case if the NEA of the surface is very small so that any scattered electron loses enough energy that it cannot be emitted. In this case, the low-energy cutoff would also be sharp as shown in Figure 5.

The only crystals investigated in-house were p-type gallium phosphide (GaP) crystals. Several attempts were made to activate thin, epitaxial layers of Zn doped GaP on GaAs substrates, but a negative-affinity surface was never achieved in the AEEA system. The high temperatures required to order the GaP surface caused disassociation of the GaAs substrates. Single crystals of GaP were purchased, but they did not arrive until after this work unit was terminated. Nevertheless, the author did successfully activate and investigate the spatial distribution of emission from these samples in a Varian LEED 240 system.[73]

The primary result of the GaP study is shown in Figure 10. Electrons were emitted with a Gaussian distribution about the surface normal. This result is consistent with a theory of near-normal photoemission from NEA surfaces first proposed by Pollard.[74] Because little effort is required in collimating or focusing a normally emitted beam, the NEA emitter has a large potential for future applications in image tubes. The major problem is increasing its lifetime in typical tube environments.

V. CONCLUSIONS

No electron source for tube applications was developed under this work unit although numerous electron filters and electron emitters were investigated. Simple electrostatic filters were used to sharpen the high-energy cutoffs in the EDC of electron emitters but were found difficult to fabricate and useful only when most of the current density of the source could be sacrificed for a sharper cutoff capable of improving a tube's contrast enhancement. Two electron emitters, miniature field-emitter tips and negative electron affinity (NEA) emitters, look promising for the future. Unfortunately, both emitters also have problems which will require further attention. The field-emitter tips can provide high current densities but suffer from excessive noise in typical tube environments. NEA emitters can provide very near normal emission but are difficult to keep stable in the long term and cannot easily provide high current densities.

---

[73] T. L. Jones, "Spatial Distribution of the Near Threshold Photoemission from (100) GaP:Cs," Masters Thesis, American Univ. (1974) (available from Xerox Univ. Microfilm, Ann Arbor, Mich).

[74] J. H. Pollard, Conference on Photoelectric and Secondary Electron Emission, Paper C. 4 (Univ. of Minn., Aug. 71) (Report available from DDC, AD #750364).

BIBLIOGRAPHY

1. Aksela, S., *Rev. of Sci. Instr.*, 42, 6, 810 (Jun 71).

2. Anderson, W. H. J., *Br. J. Appl. Phys.*, 18, 1573-9 (1967).

3. Arnow, M. and D. R. Jones, *Rev. of Sci. Instr.*, 43, 1, 72 (Jan 72).

4. Baldwin, G. C. and S. I. Friedman, *Rev. of Sci. Instr.*, 38, 4, 519 (Apr 67).

5. Bartelink, D. J., J. L. Moll, and N. I. Meyer, *Phys. Rev.*, 130, 3, 972 (1 May 63).

6. Beitel, G. A., *J. of Vac, Sci. & Tech.*, 8, 5, 647 (1971).

7. Bell, R. L., *Negative Electron Affinity Devices* (Oxford Univ. Press, London, 1973).

8. Bell, R. L. and W. E. Spicer, *Proc. of IEEE*, 58, 11, 1788 (Nov 70).

9. Biederman, H., "Electron Emission into Vacuum from Al-LiF-Au Structures," *Thin Solid Films*, 18, 1, 39 (1973).

10. Boersch, H., *Zeits. f. Physik*, 139, 115-46 (1954).

11. Bolger, D. E., "GaAsP for Low Energy Spread Cathodes," Report by Standard Telecommunications Lab on British CVD Project #RP7-68 (1971).

12. Colin, Lea, *J. Phys, D: Appl. Phys.*, "Field Emission from Carbon Fibers," 6, 1105 (1973).

13. Deasley, P. J. and K. R. Faulkner, in *Adv. in Elec. and Elec. Phys.*, Vol 33A, pp. 459-67 (Academic Press, London, 1972).

14. Di Stefano, T. H. and D. T. Pierce, *Rev. of Sci. Instr.*, 41, 2, 160 (Feb 70).

15. Faulkner, K. R., *et al.*, *Appl. Phys. Lett.*, 23, 6, 298 (15 Sep 73).

16. Fox, R. E., *et al.*, *Rev. of Sci. Instr.*, 23, 12, 1101 (Dec 55).

17. Gadzuk, J. W. and E. W. Plummer, "Field Emission Energy Distributions," *Rev. of Modern Phys.*, 45, 3, 487 (Jul 73).

18. Glascock, H. H., *Rev. of Sci. Instr.*, 43, 4, 698 (Apr 72).

19. Golden, D. E. and A. Zecca, *Rev. of Sci. Instr.*, 42, 2, 210 (Feb 71).

20. Green, T. S. and G. A. Proca, *Rev. of Sci. Instr.*, 41, 10, 1409 (Oct 70).

21. Hafner, H., J. A. Simpson and C. E. Kuyatt, "Comparison of the Spherical Deflector and Cylindrical Mirror Analyzers," *Rev. of Sci. Instr.*, 39, 1, 33 (Jan 68).

22. Harrower, G. A., *Rev. of Sci. Instr.*, 26, 9, 850 (Sep 55).

23. Holme, A. E., *et al.*, *Vacuum*, 24, 1, 7 (Oct 73).

24. Hrach, R., ". . . Emission from MIM System: Energy Distributions," *Czech. J. Phys. B.*, 18, 12, 1591 (Dec 68).

25. Hrach, R., "Emission of Electrons from MIM Structures: Discussion of Processes in the Cathode," *Czech. J. Phys. B.*, 23, 234 (1973).

26. Hughes, A. L. and V. Rojansky, *Phys. Rev.*, 34, 2, 284 (15 Jul 29).

27. Itoh, Tohru, "Energy Distribution of Electrons Emitted from Si Surface Barrier Diodes," *J. Appl. Phys.*, 41, 5, 1951 (Apr 70).

28. James, L. W. and J. L. Moll, *Phys. Rev.*, 183, 3, 740 (15 Jul 69).

29. Jones, T. L., "Spatial Distribution of the Near Threshold Photoemission from (100) GaP: Cs," Masters Thesis, American Univ. (1974) (available from Xerox Univ. Microfilm, Ann Arbor, Michigan).

30. Kohn, E. S., "Cold Cathode Electron Emission from Si," *Appl. Phys. Lett.*, 18, 7, 272 (Apr 71).

31. Kuyatt, C. E. and J. A. Simpson, "Electron Monochrometer Design," *Rev. of Sci. Instr.*, 38, 1, 103 (Jan 67).

32. Leventhal, J. J. and G. R. North, *Rev. of Sci. Instr.*, 42, 1 (Jan 71).

33. Levine, J. D., "Analysis and Optimization of a Field Emitter Array," *RCA Review*, 32, 1, 144 (Mar 71).

34. McNeil, W. D. and W. B. Shepard, "Preparation of Ge and Si Field Emission Cathodes," *Rev. of Sci. Instr.*, 43, 11, 1636 (Nov 72).

35. Marmet, Paul, *Rev. of Sci. Instr.*, 39, 12, 1932 (Dec 68).

36. Martinelli, R. U., *et al.*, RCA Final Report on USA Contract #DAAK02-71-C-0329 (Sep 72) (available from DDC).

37. Mattauch, J., *Phys. Rev.*, 50, 7, 617 (1 Oct 36).

38. Mattauch, J. and R. Herzog, *Zeits. f. Physik*, 89, 786 (1934).

39. May, J. and R. Hrach, "Emission of Electrons from MIM Systems: Angular Distributions," *Czech. J. Phys. B.*, 23, 234 (1973).

40. Mead, C. A., "Operation of Tunnel Emission Devices," *J. Appl. Phys.*, 32, 4, 646 (Apr 61).

41. Mize, J. L., "Investigation of Solid State Cold Cathodes," Final Report on USA Contract DAAK02-72-C-0163 (Jun 72) (available from DDC).

42. Mize, J. L., "Research and Fabrication of Solid State Emitter Arrays," Final Report on USA Contract DAAB02-72-C-0195 (Feb 74) (available from DDC).

43. Nasimi, M., *Rev. of Sci. Instr.*, 42, 12, 1765 (Dec 71).

44. Pollard, J. H., Conference on Photoelectric and Secondary Electron Emission, Paper C.4 (Univ. of Minn., Aug 71) (Report available from DDC, AD #750364).

45. Purcell, E. M., *Phys. Rev.*, 54, 10, 818 (15 Nov 38).

46. Risley, J. S., *Rev. of Sci. Instr.*, 43, 1, 95 (Jan 72).

47. Roy, D., *Rev. of Sci. Instr.*, 43, 3, 535 (Mar 72).

48. Roy, D. and J. D. Carette, *Rev. of Sci. Instr.*, 42, 6, 776 (Jun 71).

49. Schmidt, Conrad, *Rev. of Sci. Instr.*, 41, 1, 117 (Jan 70).

50. Schröfel, J. and I. Hüttel, *Thin Solid Films*, 21, 53 (1974).

51. Septier, Albert, ed., *Focusing of Charged Particles,* Vol. 2, Chap. IV, "Prisms" (Academic Press, N.Y., 1967).

52. Shade, H., H. Nelson, and H. Kressel, *Appl. Phys. Lett.*, 20, 10, 385 (May 72).

53. Shelton, Joe, [Oxide Metal Composite for] "Field Effect Emission," Report RN-TR-71-1, Redstone Arsenal, Alabama (Aug 71) (available from DDC).

54. Simpson, J. A., *Rev. of Sci. Instr.*, 32, 12, 1283 (Dec 61).

55. Smith, N. V. and M. M. Traum, *Phys. Rev. Lett.*, 31, 20, 1247 (12 Nov 73).

56. Spindt, C. A., "Low Energy Monoenergetic Flood Source," Final Report of USA Contract DAAK02-72-C-0144 (Sep 71) (available from DDC).

57. Spindt, C. A., "Thin Film Field Emission Devices," IEEE Conference on Elec. Device Tech., New York (1973).

58. Stolte, C. A., J. Vilms and R. J. Archer, *Sol. State Electronics,* 12, 045-54 (1969).

59. Sushkov, A. D., Russian Pat. #247427 (available from DDC-AD #743664).

60. Swank, R. K., *J. Appl. Phys.*, 41, 2, 778 (Feb 70).

61. Taheri, C. A., *et al.*, "Electrical Forming in and Electron Emission from Thin Film Aluminum-Borosilicate Glass-Aluminum Sandwiches," *Phys. Stat. Sol.*, A12, 2, 563 (1972).

62. Testerman, M. K., *et al., J. Appl. Phys.*, 36, 9, 2939 (Sep 65).

63. Thomas, R. N., *et al.*, "Fabrication and Application of Large Area Silicon Field Emitter Arrays," *Sol. State Electronics,* 17, 2, 155 (Feb 74).

64. van Laar, J., *Acta Electronica,* 16, 3, 215 (Jul 73).

65. Williams, B. F. and J. J. Tietjen, *Proc. of IEEE,* 59, 1489 (1971).

66. Williams, B. F., R. U. Martinelli and E. Kohn, in *Adv. in Elec. and Elec. Phys.*, Vol 33A, pp. 447-57 (Academic Press, London 1972).

67. Young, R. D., "Theoretical Total Energy Distribution of Field Emitted Electrons," *Phys. Rev.* 113, 1, 110 (1 Jan 59).

68. Young, R. D. and E. W. Muller, "Experimental Measurement of Total Energy Distributions of Field Emitted Electrons," *Phys. Rev.*, 113, 1, 115 (1 Jan 59).

DISTRIBUTION FOR NVL REPORT ECOM-7054

No. Copies	Addressee
12	Defense Documentation Center ATTN: DDC-TCA Cameron Station (Bldg 5) Alexandria, VA 22314
1	Director National Security Agency ATTN: TDL Fort George G. Meade, MD 20755
1	Office of Naval Research Code 427 Arlington, VA 22217
1	Director Naval Research Laboratory ATTN: Code 2627 Washington, DC 20375
1	Commander Naval Electronics Laboratory Center ATTN: Library San Diego, CA 92152
1	Commander US Naval Surface Weapons Center ATTN: Technical Library White Oak, Silver Spring, MD 20910
1	Commandant, Marine Corps HQ, US Marine Corps ATTN: Code LMC Washington, DC 20380
1	HQ, US Marine Corps ATTN: Code INTS Washington, DC 20380
1	Command, Control & Communications Div Development Center Marine Corps Development & Educ Comd Quantico, VA 22134
1	HQ ESD (XRRI) L. G. Hanscom Field Bedford, MA 01730
2	Air Force Avionics Laboratory ATTN: AFAL/TSR, STINFO Wright-Patterson AFB, OH 45433
1	AFSPCOMMCEN/SUR San Antonio, TX 78243
1	Armament Development & Test Center ATTN: DLOSL, Tech Library Eglin Air Force Base, FL 32542
1	HQDA (DACE-CMS) Washington, DC 20310
1	OSASS-RD Washington, DC 20310
1	Commander US Army Training & Doctrine Command ATTN: ATCD-SI Fort Monroe, VA 23651
1	Commander US Army Training & Doctrine Command ATTN: ATCDOCI Fort Monroe, VA 23651
1	CDR, US Army Materiel Development & Readiness Command ATTN: DRCMA-EE 5001 Eisenhower Ave Alexandria, VA 22333
1	CDR, US Army Materiel Development & Readiness Command ATTN: DRCRD-FW 5001 Eisenhower Ave Alexandria, VA 22333
1	Commander US Army Training & Doctrine Command ATTN: ATCD-F Fort Monroe, VA 23651

No. Copies	Addressee
1	Commander US Army Missile Research & Development Command ATTN: DRSMI-RR Dr. J. P. Hallowes Redstone Arsenal, AL 35809
1	Commander US Army Armament Research & Development Command ATTN: DRSAR-RDP (Library) Rock Island, IL 61201
3	Commander US Army Combined Arms Combat Developments Activity ATTN: ATCAIC-IE Fort Leavenworth, KS 66027
1	Commander US Army Logistics Center ATTN: ATCL-MA Fort Lee, VA 23801
1	Commandant US Army Ordnance School ATTN: ATSOR-CTD Aberdeen Proving Ground, MD 21005
1	Commander US Army Intelligence School ATTN: ATSIT-CTD Fort Sill, OK 73503
1	Commandant US Army Engineer School ATTN: ATSE-CTD-DT-TL Fort Belvoir, VA 22060
1	Commander Picatinny Arsenal ATTN: SARPA-TS-S #59 Dover, NJ 07801
1	Commander Frankford Arsenal ATTN: (Dr. Wm. McNeill) PDS Philadelphia, PA 19137
1	Commander USASA Test & Evaluation Center Fort Huachuca, AZ 85613

No. Copies	Addressee
1	US Army Research Office-Durham ATTN: CRDARD-IP Box CM, Duke Station Durham, NC 27706
1	US Army Research Office-Durham ATTN: Dr. Robert J. Lontz Box CM, Duke Station Durham, NC 27706
1	Commander HQ MASSTER Technical Information Center ATTN: Mrs. Ruth Reynolds Fort Hood, TX 76544
1	USA Security Agency ATTN: IARD Arlington Hall Station Arlington, VA 22212
1	Commander US Army Tank-Automotive Research & Development Command ATTN: DRSTA-RW-L Warren, MI 48090
1	Commandant US Army Air Defense School ATTN: C&S Dept, Msl Sci Div Fort Bliss, TX
1	Commander US Army Combined Arms Combat Developments Activity ATTN: ATCACC Fort Leavenworth, KS 66027
2	Commander US Army Yuma Proving Ground ATTN: STEYP-MTD (Tech Library) Yuma, AZ 85364
1	Commander US Army Arctic Test Center ATTN: STEAC-PL APO Seattle, 98733
1	CO, US Army Tropic Test Center ATTN: STETC-MO-A (Technical Library) Drawer 942 Fort Clayton, Canal Zone 09827

No. Copies	Addressee
1	Commander US Army Logistics Center ATTN: ATCL-MC Fort Lee, VA 22801
1	Directorate of Combat Developments US Army Armor School ATTN: ATSB-CD-AA Fort Knox, KY 40121
1	Commandant US Army Inst for Military Assistance ATTN: ATSU-CTD-OMS Fort Bragg, NC 28307
1	Commander US Army Missile Research & Development Command ATTN: DRSMI-RE (Mr. Pittman) Redstone Arsenal, AL 35809
1	Commander US Army Systems Analysis Agency ATTN: (Mr. A. Reid) DRXSY-T Aberdeen Proving Ground, MD 21005
1	Commandant US Army Signal School ATTN: ATSN-CTD-MS Fort Gordon, GA 30905
1	Commander US Army Tank-Automotive Research & Development Command ATTN: DRSTA-RHP Dr. J. Parks Warren, MI 48090
2	NASA Scientific & Tech Info Facility ATTN: Acquisitions Branch (S-AK/DL) P.O. Box 33 College Part, MD 20740
2	Advisory Group on Electron Devices 201 Varick St, 9th Floor New York, NY 10014

No. Copies	Addressee
1	Ballistic Missile Radiation Anal Ctr Env Research Inst of Michigan Box 618 Ann Arbor, MI 48107
2	Chief Ofc of Missile Electronic Warfare Electronic Warfare Lab, ECOM White Sands Missile Range, NM 88002
1	Chief Intel Materiel Dev & Support Ofc Electronic Warfare Lab, ECOM Fort Meade, MD 20755
2	Commander US Army Electronics Research & Development Command ATTN: DRSEL-MS-TI Fort Monmouth, NJ 07703
1	TACTEC Battelle Memorial Institute 505 King Avenue Columbus, OH 43201
1	Commander US Army Electronics Research & Development Command ATTN: DRSEL-PL-ST Fort Monmouth, NJ 07703
1	Study Center National Maritime Research Center ATTN: Rayma Feldman King's Point, NY 11024
1	Infrared Info & Analysis Center P.O. Box 618 ATTN: Library Ann Arbor, MI 48107
1	Defense Communication Agency Tech Library Ctr Code 205 Washington, DC 20305
1	Environmental Res Inst of Michigan P.O. Box 618 Ann Arbor, MI 48107
25	Night Vision Laboratory DRSEL-NV Fort Belvoir, VA 22060

12 69,398—AG—Ft Belvoir